

OSIRIS-REx Camera Suite Calibration Description

OSIRIS-REx DOCUMENT

Rev_1.7

10/10/2019

Prepared by Dathon Golish and Bashar Rizk





CM FOREWORD

This document is an OSIRIS-REx Project controlled document. Changes to this document require prior approval of the OSIRIS-REx Configuration Control Board (CCB) and Configuration Management Lead (CML). Proposed changes shall be submitted to the OSIRIS-REx Project CML, along with supportive material justifying the proposed change.

Questions or comments concerning this document should be addressed to:

SPOC Configuration Management Team
1415 N. 6th Avenue
Tucson, AZ 85705

Email: spoc-cm@orex.lpl.arizona.edu



DOCUMENT CHANGE LOG

Version	Description of Change/Remarks
1.6	Internal draft of charge smear changes
1.7	Section 2.4 - Update of charge smear description to make more general rather than EGA specific.
1.7	Convert document to OSIRIS-REx document format
1.7	Addition of Appendix A - Settings file usage



TABLE OF CONTENTS

CM FOREWORD.....	2
DOCUMENT CHANGE LOG.....	3
TABLE OF CONTENTS	4
LIST OF FIGURES	4
LIST OF TABLES.....	4
ABBREVIATIONS AND ACRONYMS.....	6
1 Introduction.....	7
1.1 OCAMS Overview	7
2 Nominal OCams calibration	8
2.1 Bias (1112x1044 array size).....	9
2.2 Dark (1112x1044 array size)	11
2.3 Bias + Dark (1112x1044 array size).....	12
2.4 Charge Smear.....	12
2.5 Flat Field (1024x1024 array size).....	15
2.6 Laboratory Radiometric Calibration to Radiance (Rad 250-1100nm) (1024x1024 array size)	15
2.7 Radiometric Calibration to Radiance (1024x1024 array size).....	16
2.8 Radiometric Calibration to Spectral Radiance (1024x1024 array size).....	16
2.9 Radiometric Calibration to Reflectance (I/F).....	18
3 Availability of Calibration Files on SPOCflight.....	20
Appendix A – Usage of the OCAMS Calibration Settings File.....	21

LIST OF FIGURES

Figure 1 Flowchart of OCAMS Pipeline Processing	8
Figure 2 OCAMS CCD Region Layout.....	9

LIST OF TABLES

Table 1-1: Abbreviations and Acronyms.....	6
--	---



Table 2-1 OCAMS Radiance Responsivities to reflected solar light between 250 and 1100 nm in (DN/sec / Wm ⁻² sr ⁻¹)	16
Table 2-2 OCAMS Panchromatic Filter Radiance Responsivities to reflected solar light within the band (DN sec ⁻¹) / W m ⁻² sr ⁻¹)	16
Table 2-3 OCAMS MapCam Color Filter Spectral Radiance Responsivities to reflected solar light within the band (DN sec ⁻¹) / (W m ⁻² μm ⁻¹ sr ⁻¹)	17
Table 2-4 Thermal-spectral responsivity dependence	17
Table 2-5 Solar Irradiances (W m ⁻²) used in converting to I/F	18
Table 2-6 OCAMS Solar Irradiances (W m ⁻² μm ⁻¹) used in converting to I/F	19



ABBREVIATIONS AND ACRONYMS

Table 1-1: Abbreviations and Acronyms

Phrase/Acronym	Description
CCD	Charge Coupled Device
DA	Detector Assembly
DN	Digital Number
FITS	Flexible Image Transport System
FM	Flight Model
FPA	Focal Plane Array
IDL	Interactive Data Language
L0	Level 0
L1	Level 1
L2	Level 2
MATLAB	Matrix Laboratory
OCAMS	OSIRIS-REx Camera Suite
PDS	Planetary Data System
PTC	Photon Transfer Curve
RCC	Radiometric Calibration Constant
SIS	Software Interface Specification
SNR	Signal to Noise Ratio
SPOC	Science Processing and Operations Center
TVAC	Thermal Vacuum
UUT	Unit Under Test



1 INTRODUCTION

The Origins, Spectral Interpretation, Resource Identification, Security – Regolith Explorer (OSIRIS-REx) mission will return the first pristine samples of carbonaceous material from the surface of a primitive asteroid. OSIRIS-REx's target asteroid (101955) Bennu is the most exciting, accessible, volatile, and organic-rich remnant from the early solar system, as well as one of the most potentially hazardous asteroids known.

After launching in September 2016, OSIRIS-REx undergoes a two-year cruise to Bennu that includes an Earth flyby in September of 2017. OSIRIS-REx detects Bennu 60 days in advance of rendezvous and surveys its environment for natural satellites and other hazards. OSIRIS-REx then spends the next months characterizing the surface and orbital environment of Bennu. Primary and backup sample sites are characterized with OSIRIS-REx's instrument suite and the Touch-And-Go (TAG) maneuver sequence is practiced. In July 2020, OSIRIS-REx executes the TAG maneuver and collects both bulk and surface samples. After a period of quiescent drifting away from Bennu, in March of 2021, OSIRIS-REx begins its return journey to the Earth. Following a 2.5 year return cruise, the Sample Return Capsule (SRC) is released, re-entering Earth's atmosphere and landing at the Utah Test & Training Range in September of 2023.

1.1 OCAMS Overview

The OSIRIS-REx Camera Suite (OCAMS) is a set of three cameras designed to support the mission through all phases, from approach to sample collection. The asteroid is first acquired through the PolyCam, an 8" Ritchey-Chretien telescope capable of detecting up to 12th magnitude objects limited by spacecraft jitter. As features on the asteroid become resolvable, PolyCam is used for preliminary mapping at a surface resolution of <25 cm. MapCam performs mapping at a suite of phase angles using a panchromatic and four color filters. The asteroid sampling sequence is documented by the widefield SamCam and gives the context for the recovered sample. All cameras use identical detector arrays with different focal lengths separated by a factor of 5. Data processing and calibration of the camera suite's images is also identical in terms of algorithms, however specific calibration coefficients are applied on a per-camera basis. This document describes the OCAMS data processing pipeline calibration algorithms and the application of relevant calibration coefficients.



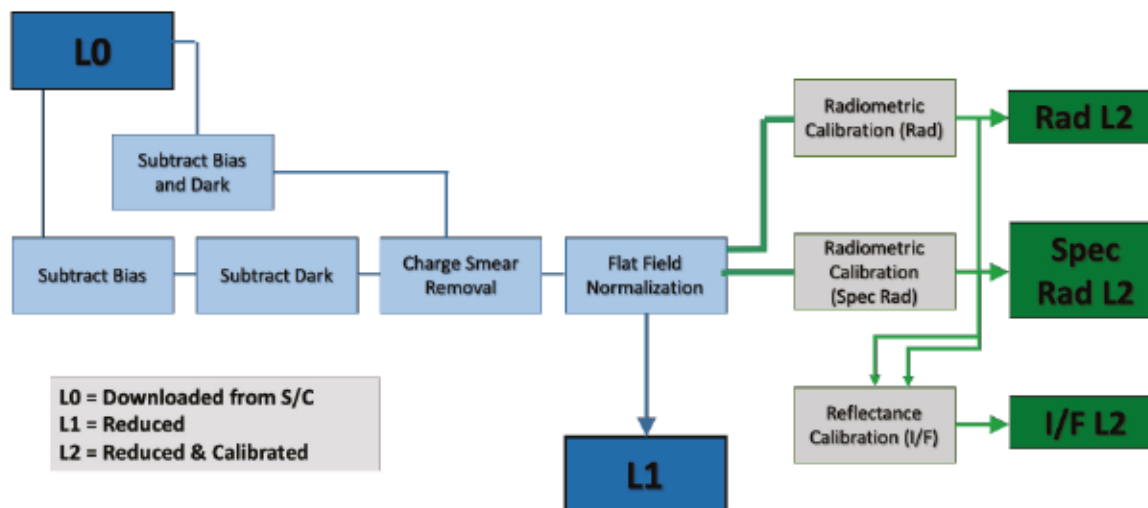
2 NOMINAL OCAMS CALIBRATION

OCAMS images acquired in flight and provided through the PDS experience several processing steps that convert the raw signal recorded in DN by the instruments in flight to the signal archived by the data repository. They begin life as electronically shuttered images recorded during the mission as individual electrons that correspond to the solar photons reflected from the surface of the Bennu, the Earth, the Moon, the planets and main-belt asteroids or as stellar photons from any of several thousand distant stars

These processing steps are described below within individual sections. In summary they consist of bias/dark subtraction, charge-smear correction, flat-field normalization to convert the raw L0 images transmitted from the spacecraft and provided by the ground data system to L1 FITS files. Radiometric calibration converts L1 files into several different flavors of L2 (Figure 1), including a radiance (Rad), a spectral radiance (Spec Rad) and a reflectance (I/F) product. Versioning of the OCAMS pipeline is recorded in each image label in the Mission_area data_processing_information class `ocams_pl_ver` attribute.

More extensive descriptions will be provided when the OCAMS team publishes the calibration of the OCAMS instruments, a process that is still on-going. A full instrument description can be found in Rizk et al., 2018.

Figure 1 Flowchart of OCAMS Pipeline Processing

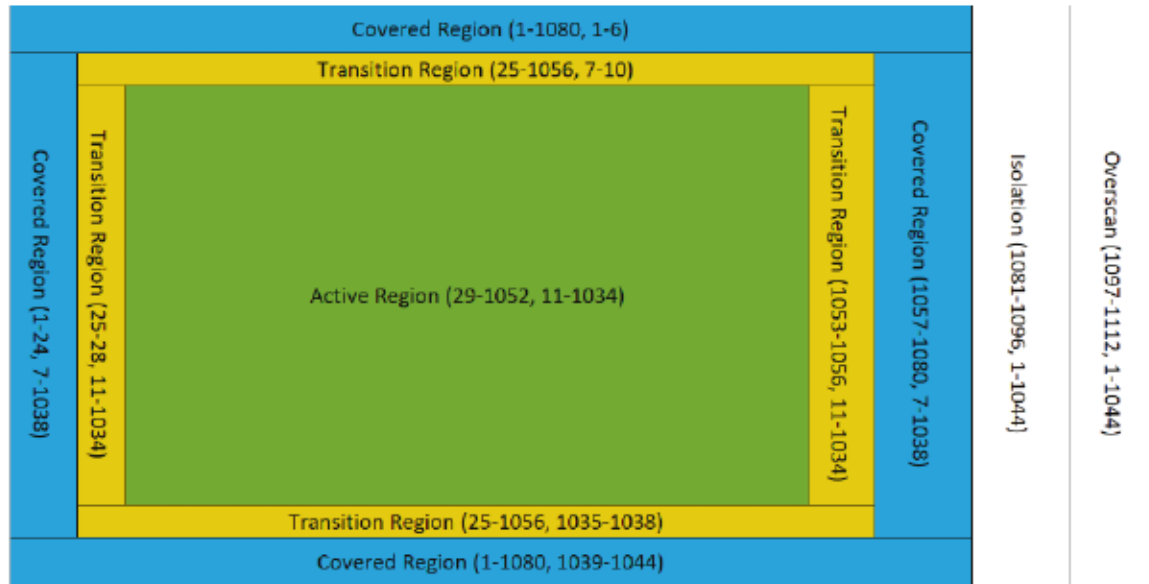


Some processing steps will refer to regions of the image that are used to correct the images. Those regions include the 1024x1024 active region (the image being corrected), the covered regions (physically CCD pixels that are masked and are not exposed to light), and overscan regions (virtual pixels that are created when the electronics perform empty reads at the end of each row). The transition and isolation regions are buffers between other



regions to prevent signal leakage between them. The regions are shown in Figure 2 for reference. Read noise in the instrument is approximately 10 DN (Rizk et al. 2018). The calibration pipeline operates on the full image array unless otherwise stated.

Figure 2 OCAMS CCD Region Layout



2.1 Bias (1112x1044 array size)

Bias subtraction is intended to remove the fixed offset applied by the readout electronics. A bias subtracted image (in the absence of dark or optically generated current) should have a mean value of 0.

Bias subtraction is applied in the following way:

A master bias file (1112x1044) is created from bias images taken either on the ground or coincident with the images being corrected. The master bias file used is recorded in the reference list section of the data product label. The algorithm performs pixel-wise subtraction (e.g. a straight array subtraction) of the master bias file (*Bias*) from the image being processed (*Raw*), as shown in Equation 1.

$$Tmp_{ij} = Raw_{ij} - Bias_{ij} \quad (1)$$



After subtracting the master bias, to account for bias variations at the moment of acquisition, overscan columns are used to update the bias correction. The overscan columns are not physical pixels; they are empty reads of the readout electronics, which should contain only the bias offset plus read noise. The overscan columns are the last 16 columns read out by the detector. The overscan columns having been corrected by Equation 1, the master bias, so any residual signal should be the in-situ bias variation. To correct for the in-situ variation, the median of the 16 overscan columns (see Figure 1) are taken on a row-wise basis and then the column vector of the results is box-car smoothed¹. The size of the kernel is user controllable, but the default is 51 pixels. This large default is chosen to smooth the impact of extended cosmic ray hits that can cover several pixels. Although cosmic ray hits cannot affect the overscan columns, this operation is kept consistent with the Dark and Bias/Dark algorithms (which can be affected by cosmic rays). The smoothed result is subtracted on a row-wise basis, as shown in Equations 2-4.

$$\text{overscan}_i = \text{median}\{T_{mp_{i,1}} \dots T_{mp_{i,24}}, T_{mp_{i,1057}} \dots T_{mp_{i,1080}}\} \quad (2)$$

$$\overrightarrow{\text{overscan}}' = \text{boxcar}(\overrightarrow{\text{overscan}}, 51) \quad (3)$$

$$\overrightarrow{\text{Corrected}}_i = \overrightarrow{T_{mp}_i} - \overrightarrow{\text{overscan}}' \quad (4)$$

¹ The standard IDL function SMOOTH is applied, using the EDGE_TRUNCATE option. The IDL SMOOTH function returns a copy of the input array smoothed with a boxcar average of the specified full width

$$W = \begin{cases} \text{width} & \text{if width is odd} \\ \text{width} + 1 & \text{otherwise} \end{cases}$$

We use the "EDGE_TRUNCATE" option, under which the edge pixels are assumed to be replicated as many times as necessary to complete the boxcar. The equation is thus:

$$R_i = \frac{1}{W} \sum_{j=0}^{W-1} A_{i+j-\text{floor}(\frac{W}{2})}$$

Where A_k is taken as the edge pixel A_0 or A_{N-1} if the subscript quantity $k = i + j - \text{floor}(\frac{W}{2})$ is < 0 or $> N - 1$, respectively



2.2 Dark (1112x1044 array size)

Dark subtraction removes the signal generated not by photons, but by phonons, thermal excitations in the detector material. Dark signal is removed in a way similar to bias signal:

A master dark file (1112x1044) is created from dark images taken coincident with the images being corrected. The master dark file used is recorded in the reference list section of the data product label. The algorithm performs pixel-wise subtraction (e.g. a straight array subtraction) of the master dark file (*Dark*) from the image being processed (*Raw*), as shown in Equation 5. The advantage to this method is that it corrects pixel-to-pixel variation in the dark current, which can vary across the detector. Note that the input to this process has likely been bias corrected, but is referred to here as *Raw*, without that assumption.

$$Tmp_{ij} = Raw_{ij} - Dark_{ij} \quad (5)$$

After subtracting the master dark, to account for dark current variations at the moment of acquisition, covered columns are used to update the dark correction. There are 24 covered columns on either side of the active region (48 columns total, indicated in blue on Figure 1). Because the covered columns are physical pixels, they are susceptible to both hot pixels and cosmic ray hits. To prevent their contribution to the correction, the covered columns are scrubbed for bad pixels. Bad pixels are identified as those pixels that are statistically different than their neighbors. Specifically, the mean and standard deviation are calculated for a 10x10 pixel window and pixels that are more than 5 standard deviations higher than the mean are identified as bad. The 10x10 pixel window is swept across the covered columns in 5 pixel steps to find all bad pixels using their local statistics. Bad pixels are corrected by replacing their value with the mean of their 4 nearest neighbors. The covered columns have themselves been corrected by the master dark; any residual signal in those columns represent instantaneous dark current variation. To correct for that variation, the median of the 48 covered columns are calculated on a row-wise basis and then the column vector of the results is box-car smoothed as with bias correction. The smoothed result is subtracted on a row-wise basis, as shown in Equations 6-8.

$$covered_i = median\{Tmp_{i,1} \dots Tmp_{i,24}, Tmp_{i,1057} \dots Tmp_{i,1080}\} \quad (6)$$

$$\overrightarrow{covered}' = boxcar(\overrightarrow{covered}, 51) \quad (7)$$

$$\overrightarrow{Corrected}_i = \overrightarrow{Tmp}_i - \overrightarrow{covered}' \quad (8)$$



2.3 Bias + Dark (1112x1044 array size)

For the majority of the OCAMS images taken in flight, even star fields, bias levels have dominated the dark current, which is measurable but rather inconsequential. As a result, the bias + dark correction can be conveniently and effectively applied together. The master bias+dark files (1112x1044) are tagged with the time period and exposure time for which they are relevant and used to process images acquired within that period and with identical exposure times. The combined BiasDark calculation is performed in the same way as with the bias and darks individually (i.e. subtract BiasDark master and then update via covered columns using Equations 6 - 8).

2.4 Charge Smear

Charge smear is the result of signal being generated when exposed to light during the frame transfer of pixel wells both on and off the active area. It is most noticeable when a very bright object, whether point source or extended source, is resident within the camera's field of view, requiring a very short exposure time. The exposure time is short enough to be comparable to the time required to clock the pixels on and off the array. As a result, an extended line is recorded above and below the bright source, marking the charge collected by each of these pixels as a bright object's image is trailed across them. In order to be radiometrically accurate, removing charge smear signal requires reducing the effective exposure time of the image. This effective exposure time (found in the L1 reduced image product in the `effective_exposure` attribute), calculated as the actual exposure time subtracted by the frame transfer time (1.044 ms, with a row transfer time of 1 μ s) is tracked in the header (`EXPEFF`) of the FITS file and used directly by the radiometric corrections later in the pipeline. Note that images with exposure times longer than 100 ms generally will not be corrected for charge smear, as charge smear at this point contributes less than 1% additional signal to the image and the correction is more likely to introduce noise than correct it. There are specific instances where these images will be charge smear corrected. See Appendix A for information on how to identify these instances.

The signal recorded by the detector due to the full imaging operation (exposure time and frame transfer time) can be measured by summing the signal on a column-wise basis. This sum is the full amount of charge accumulated. A fraction of that charge (the ratio of the row transfer time to the integration time) will be distributed to each pixel in the column. A first order correction for charge smear is to subtract that fraction of the total signal off of every pixel in a given column. However, this correction is an overestimate because it includes the signal generated by charge smear itself. We can solve for the true amount of charge smear in the following way. The total signal measured by a given pixel is the combination of the true signal from its location in the scene and the charge smear from locations above and below it.

$$S = \hat{S} + E \quad (9)$$



where \mathbf{S} is the measured signal, $\widehat{\mathbf{S}}$ is the actual signal, and \mathbf{E} is the contribution from charge smear. For pixel (i,j) , the charge smear contribution is proportional to the sum of the actual signals in that column.

$$S_{i,j} = \widehat{S}_{i,j} + \epsilon \sum_i \widehat{S}_j \quad (10)$$

where (i,j) is the (row, column) of the pixel location and ϵ is the ratio of row transfer time to exposure time (i.e. how long each pixel is exposed to the other locations in the scene as the frame is transferred). The signal measured in a column is then the sum of all pixels in that column.

$$\sum_i S_j = \sum_i (\widehat{S}_{i,j} + \epsilon \sum_i \widehat{S}_j) \quad (11)$$

$\sum_i S_j$ is the sum of the j^{th} column in the image. It is an input to the solution, so will be represented as the variable \mathbf{Y} . We substitute this in, as well as substituting $\widehat{\mathbf{S}} = \mathbf{S} - \mathbf{E}$.

$$Y_j = \sum_i ((S_j - E_j) + \epsilon \sum_i (S_j - E_j)) \quad (12)$$

Again we can substitute the measured signal in the column, \mathbf{Y} .

$$Y_j = \sum_i (S_j - E_j + \epsilon Y_j - \epsilon \sum_i E_j) \quad (13)$$

The sum of the charge smear term over the column is merely the charge smear term, summed N_{row} times (the number of rows, 1044).

$$\sum E = N_{\text{row}} * E \quad (14)$$

We can therefore substitute further and distribute the summing operation.

$$Y_j = \sum_i S_j - \sum_i E_j + \sum_i \epsilon Y_j - N_{\text{row}} * \epsilon \sum_i E_j \quad (15)$$



$$Y_j = Y_j - N_{row} * E_j + N_{row} * \epsilon * Y_j - N_{row}^2 * \epsilon * E_j \quad (16)$$

Finally, we can solve for the charge smear term, which will convert the measured signal of any pixel in the j^{th} column to the actual signal.

$$E_j = \frac{\epsilon Y_j}{N_{row}\epsilon + 1} \quad (17)$$

In practice, we have seen that this does not perfectly correct charge smear. To improve the correction, we use the covered rows to evaluate the residual. If the above algorithm perfectly predicted charge smear, the covered rows would have a mean signal of zero (assuming bias and dark signals have already been removed). Mean signal above or below zero in the covered rows indicate under- or over-correction in the charge smear algorithm. We can therefore modify the magnitude of the correction in the appropriate direction and repeat the correction. This continues iteratively until the mean signal in the covered row region is minimized (i.e. iterate correction by 1% steps until an error inflection is reached. The correction with the minimum error value is used). This method is less susceptible to the small number of covered rows, because we can average all the columns together to improve our statistics. The iterative algorithm leads to near complete removal of charge smear. This iterative method of charge smear correction is the default method and is referred to as the 'HYBRID' method in the settings file. Note that the magnitude of the correction the needs to be applied to the charge smear vector when iterating can be large, e.g. on the order of 0.1 (10x) in very low exposure images.

For images where the target does not fill the full field of view, an alternative charge smear correction method was necessary due to very short exposure times (see the EGA 'Icicles' phenomenon in the OCAMS EGA Caveats Document). One of two methods are used, both of which require user intervention to choose a portion of the image to use to generate the correction. In the 'GUIDED' method, the user provides the row and column values for the four corners of a rectangle that contain only charge smear (e.g. off the limb of the Earth/Moon/Bennu, looking at dark sky). The median (along the columns) of the pixels within that rectangle are used to create a correction vector that is subtracted off of the entire image. Columns outside the rectangle will have a correction of zero. The 'INSITU' method is used for images (currently only EGA) that do not have any dark sky in the image. The user provides the starting and ending columns (the row values are ignored and can be provided as zeros) of a region of the image that has a relatively uniform scene (e.g. uniform clouds). The intention is that the variation in this uniform region is representative of charge smear and can be used to generate a correction. Clearly this method can only be as effective as the uniformity of the background, but there are some EGA images for which this



is the only option. The median of the rows indicated by the column limits is calculated to create a column-wise charge smear correction.

The methods and values used for all charge smear corrections are provided in the OCAMS pipeline calibration settings file (`ocams_pl_cal_settings.csv`) provided in the calibration collection of the OCAMS bundle. Use of this file is described in Appendix A.

2.5 Flat Field (1024x1024 array size)

Flat field corrects for the spatial variation in optical responsivity across the detector itself. It can account for both slowly varying and rapidly-varying (pixel-to-pixel) relative responsivities. It is currently only corrected by applying a master flat field acquired on the ground. The master flat field (1024x1024) used is indicated in the data product label reference list. The master flat field is calculated as the inverse of the system response to a spatially uniform scene. Therefore, the master flat field (*Flat*) is applied by multiplying it against the image to be corrected (*Raw*), as shown in Equation 18. Note that the input to this process has likely been bias/dark corrected, but is referred to here as *Raw*, without that assumption.

$$Corrected_{ij} = Raw_{ij} * Flat_{ij} \quad (18)$$

2.6 Laboratory Radiometric Calibration to Radiance (Rad 250-1100nm) (1024x1024 array size)

Radiometric calibration to radiance converts the signal rate in DN/sec between 250 and 1100 nm to the radiance of the detected field in $W m^{-2} sr^{-1}$ by applying radiometric calibration constants determined on the ground. These conversions were used for laboratory calibrations during ground testing. These constants are expressed in terms of signal, per second, per unit of radiance. Therefore, to convert to radiance, the measured signal (*DN*) is divided by the radiometric calibration constant (*RCC*) and by the effective exposure time (t_{exp}) of the image, as shown in Equation 19. The effective exposure time, as described in the Charge Smear section, is recorded in milliseconds. However, the RCC is calculated in terms of seconds, so the effective exposure time must be converted to seconds before use in Equation 19. The RCC is temperature-dependent, so is scaled based on the temperature of the CCD at the time of image acquisition (see Equation 21).

$$Radiance_{ij} = \frac{\left(\frac{DN_{ij}}{t_{exp}}\right)}{RCC} \quad (19)$$



Table 2-1 OCAMS Radiance Responsivities to reflected solar light between 250 and 1100 nm in (DN/sec / Wm⁻²sr⁻¹)

MapCam	Pan	Pan-30	b	v	w	x
	379000	385000	44600	54800	74000	51100
PolyCam	Pan					
	271000					
SamCam	Pan 1	Pan 4	Pan 5	Diopter		
	128000	129000	128000	13000 0		

2.7 Radiometric Calibration to Radiance (1024x1024 array size)

For the panchromatic filters, radiometric calibration to radiance converts the signal rate in DN/sec to radiance detected in W m⁻² sr⁻¹ at the band center of each of the filtered optical pathways possessed by the OCAMS instruments, as shown in Equation 19.

Table 2-2 OCAMS Panchromatic Filter Radiance Responsivities to reflected solar light within the band (DN sec⁻¹) / W m⁻² sr⁻¹)

MapCam	Pan	Pan-30			
	761000	761000			
PolyCam	Pan				
	556000				
SamCam	Pan 1	Pan 4	Pan 5	Diopter	
	255000	258000	255000	260000	

2.8 Radiometric Calibration to Spectral Radiance (1024x1024 array size)

For the color filters, radiometric calibration to spectral radiance converts the signal rate in DN/sec to spectral radiance in W m⁻² μm⁻¹ sr⁻¹ at the band center of each of the filtered optical pathways possessed by the OCAMS instruments, as shown in Equation 19.



Table 2-3 OCAMS MapCam Color Filter Spectral Radiance Responsivities to reflected solar light within the band (DN sec⁻¹) / (W m⁻² μm⁻¹ sr⁻¹)

MapCam	b	v	w	x
	22900	29900	52900	51900

As with all silicon-based detectors, the responsivity of the OCAMS CCDs are thermally dependent and that dependence is coupled with wavelength. The responsivities listed above for the OCAMS cameras were measured at room temperature, but flight operations will take place at colder temperatures. As such, responsivity has a linear temperature dependence for each filter. When OCAMS images are converted to radiance, the responsivity term is first adjusted for this dependence, listed in Table 2-4 Thermal-spectral responsivity dependence.

Table 2-4 Thermal-spectral responsivity dependence

Camera / Filter	Thermal-spectral responsivity slope (°C ⁻¹)	Reference Temperature (°C)
MapCam / b'	-0.0014	30.2
MapCam / v	-0.00075	30.0
MapCam / w	0.00053	30.1
MapCam / x	0.003	26.6
MapCam / pan	0.00075	28.6
PolyCam / pan	0.00075	27.2
SamCam / pan	0.00075	29.6

$$tsr' = (1 + (T_{ccd} - T_{ref}) * tsr) \tag{20}$$

$$RCC' = RCC * tsr' \tag{21}$$

where T_{ccd} is the temperature of the CCD (MCCCDTMP, PCCCDTMP or SCCCDTMP label attribute) at the time of the image, T_{ref} is the temperature at which the nominal responsivity was measured, tsr is the slope of the temperature-spectral responsivity dependence, RCC (see Eq. 19) is the nominal responsivity for that filter at the reference



temperature, and RCC' is the adjusted responsivity. Radiance calculated using RCC' is the responsivity reported in the OCAMS L2 data products.

2.9 Radiometric Calibration to Reflectance (I/F)

From the values in Table 2-1 and Table 2-3, combined with the solar irradiance standards displayed in Table 2-5, the I/F of each observed surface can be produced using the relationship:

$$\frac{I}{F} = L * \pi * \frac{D_{sun}^2}{F_{band}} \quad (22)$$

where

r is the range to the Sun (AU); this is derived from the mission profile, usually passed through the image header which uses the tool `spatialgen` to produce the range

t is the integration time (sec);

I is the intensity (radiance), or spectral radiance, measured within a band at the pixel (either $Wm^{-2} sr^{-1}$ or $Wm^{-2} sr^{-1}\mu m^{-1}$) depending upon whether one is considered panchromatic data (the former) or colored filter bandpass data (the latter) (I/F is provided within the L2 image);

L is the radiance measured by the OCAMS detector within the band at the pixel ($W/m^2/sr$ or $W/m^2/sr/\mu m$);

F_{band} is the Sun's irradiance or spectral irradiance within the band at 1 AU illuminating the surface at the location of the pixel (See Table 2-5 and Table 2-6).

Table 2-5 Solar Irradiances ($W m^{-2}$) used in converting to I/F

MapCam	Pan & Pan-30
	501.049
PolyCam	Pan
	490.6251
SamCam	Pan 1, 4, 5, Diopter



504.3337

Table 2-6 OCAMS Solar Irradiances ($W\ m^{-2}\ \mu m^{-1}$) used in converting to I/F

MapCam	b	v	w	x
	2003.167	1837.798	1426.860	993.7742

It should be noted that the calculation of the L2 I/F images (in units of reflectance) depends on the amount of solar flux incident on the surface, which in turn depends on the distance from the Sun to the target. In the OCAMS calibration pipeline, the distance used is the distance from the Sun to the OSIRIS-REx spacecraft (sc2sun_range_km label attribute, SCSUNRNG FITS header keyword), which will be slightly different. However, for even the earliest resolved images of Bennu, the difference between the two distances is $< 0.1\%$. For all of Proximity Operations, the difference is $< 0.00001\%$. The only other target for which reflectance is meaningful is the Moon during the Earth Gravity Assist. For the Moon images on 09/25/2017, which have been used to radiometrically verify the cameras, the difference is $\sim 0.5\%$. For the Moon images on 10/02/2017, the difference is $\sim 3\%$. However, in these images the Moon subtends only a few pixels, therefore it is not expected that those data will ever be used for radiometry. As a result, the OCAMS calibration pipeline will not be changed to use distance-to-target in the calculation of the I/F L2 images.



3 AVAILABILITY OF CALIBRATION FILES ON SPOCFLIGHT

Internally, calibration files are distributed to the team in a convenient fashion by making them available on SPOCFlight. On this system, one selects

Engineering→Calibrations→Select Instrument→ocams, Select Calibration→ (one of several choices). They are time-tagged with a Start and Stop Date (e.g., 20160301100000 for yyymmddhhmmss) to delimit the time period over which they are intended to apply.

These files are available to PDS users in the OCAMS Bundle Calibration collection. Files used to correct a particular image are listed in that image's label reference list.



Appendix A – Usage of the OCAMS Calibration Settings File

The OCAMS Calibration Settings file is a comma separated variable file that provides time ranges for settings used in the pipeline data processing. The settings indicate which algorithms were performed in which order on the images, as well as setting any variables for specific algorithms. With very few exceptions, the pipeline algorithm order and execution have remained the same over the course of the mission. The columns that describe the order or execution of pipeline algorithms are the “do” columns (i.e DOBIAS, DODARK, DOCHSM, DOFLAT etc.) One exception in the order and execution of the pipeline was a time period between 09/11/2018 and 10/14/2018 where the charge smear algorithm was disabled for the collection of dust plume search images and for approach images with exposure times greater than 100ms. It was at this time that a new setting was introduced to the setting file to allow the charge smear exposure threshold (EXPTHRS) to be a settable parameter. Prior to 09/11/2018 images longer than 100ms were not charge smear corrected. If parameters are changed, a note will be made in the description column of the settings file.

The charge smear method applied to each image is recorded in the CHSMETHOD column. The options in this column are COVROW, HYBRID, GUIDED, or INSITU. The COVROW option is legacy, does not perform well and is therefore not expected to be used during encounter. The pipeline calibration settings file contains the row and column start/stop designations needed for the indicated charge smear method. To use the pipeline calibration settings file for the charge smear variable, find the image mid-observation acquisition time in the image label (mid_obs). Open the settings file and find the camera of interest (map, poly, sam in column 1 of the settings file) and a time range of start and stop times (columns 2 and 3 of the settings file) that contain the image acquisition time. All settings on the corresponding row have been applied to that image. Blank cells in the row indicate that either the corresponding algorithm was not performed, or the setting was not used. If the image acquisition time is not included within the time ranges of any entry, the mission-wide default values are used. These values are found as the first entries in the file, with start and end dates of 2015-01-01T00:00:00.000 to 2050-01-01T00:00:00. The description field in the record gives the effective times of these default values. The effective times are processing times rather than acquisition times. To find the appropriate mission-wide default set, find the spoc_date attribute in the image label and use the mission-wide entry that contains the spoc_date time within the effective range and is for the appropriate camera.